Laser instabilities in homogeneously broadened dense media

Michael Fromager,* Marc Brunel, and François Sanchez†
Groupe d'Optique et d'Optronique, CORIA, UMR 6614, Université de Rouen, Place Emile Blondel, 76821 Mont-Saint-Aignan Cedex, France
(Received 22 December 1999; published 10 April 2000)

We investigate the laser equations in the mean-field limit for a homogeneously broadened two-level system, taking into account the local-field correction arising from dipole-dipole interactions. Our analysis concentrates on the dynamical properties of the laser versus the pumping parameter. The effect of detuning between atomic and cavity frequencies is also studied. We first show that the local-field correction reduces the range of the chaotic regime when the frequency detuning is set for minimum instability threshold operation. For a fixed local-field correction, we demonstrate that the symmetry of the dynamical scenario versus the frequency detuning is broken. In addition, we point out generalized bistability between the chaotic regime and the off state of the laser. This bistability results from the smallness of the basins of attraction of the off state.

PACS number(s): 42.55.−f, 42.60.Mi, 42.65.Sf, 42.65.Pc

I. INTRODUCTION

The interest in laser instabilities has been growing during the two past decades. This field of investigation was initially opened by Haken, who established the fundamental analogy between single-mode homogeneously broadened laser equations and Lorenz equations [1], thus demonstrating that deterministic chaos was possible in laser systems. These equations predict chaos in the bad-cavity and high-intensity domain through a Hopf bifurcation. Much attention has been given to the influence of the microscopic parameters and decay times on the instability threshold [2–6] and more generally on the dynamical properties of the solutions [2–8]. The nature of the bifurcation (subcritical or supercritical) has been investigated in [3,5]. The effect of detuning between the atomic and cavity frequencies on the dynamics has also been investigated [2]. The main result is that the introduction of detuning destroys much of the complicated behavior of the real Lorenz-Haken equations and has a stabilizing effect. However, the frequency detuning increases the value of the instability threshold [2,6]. The latter can be significantly lowered by taking into account some inhomogeneous broadening process [9]. More recently, we have demonstrated that the local-field correction (LFC) substantially reduces the instability threshold in a homogeneously broadened single-mode laser [10]. The LFC resulting from dipole-dipole interactions has been considered previously in connection with intrinsic optical bistable media [11–17]. The influence of the LFC on laser instabilities in inhomogeneously broadened media had also been reported [18]. Again, the LFC reduces the instability threshold. The aim of this paper is to investigate the effects of dipole-dipole interactions on the dynamical properties of a detuned single-mode homogeneously broadened laser.

It has been shown that the LFC leads to a direct coupling between the population inversion and the macroscopic polarization [13,15] and can be viewed as a renormalization of the frequency detuning. One can therefore expect that the role of the LFC will be equivalent to an additional frequency detuning. In fact, we will demonstrate that this is true in the stationary regime but it is no longer valid in the time-dependent regime achieved when the steady state is unstable. Our paper is organized as follows. In Sec. II we give the modified Maxwell-Bloch equations and transform them into a more convenient form for both numerical integration and representation of the different attractors. We also emphasize the symmetry properties of the equations versus the frequency detuning. Note that, in the absence of LFC, the solutions of the detuned laser equations do not depend on the sign of the detuning [2,19]. Section III is devoted to the stationary states of the laser equations. It appears that the LFC leads to the existence of two lasing steady-state solutions [10]. This is connected to intrinsic optical bistable properties exhibited by dense media in single-pass processes [11,12]. In Sec. IV, we perform a linear stability analysis of the steady-state solutions. In particular, we demonstrate that the off state becomes stable again above the lasing threshold of the upper lasing solution, which is always unstable. The first lasing solution is stable from the threshold to a critical value of the pumping parameter for which the system loses its stability through a Hopf bifurcation [10,20,21]. In Sec. V, we numerically solve the nonlinear coupled differential equations. We focus our interest on pointing out features induced by the local-field correction. We first show that the LFC reduces the chaotic domain when the detuning is set to achieve a minimum instability threshold operation. The effect of the detuning appears to be very different from what it is in the laser equations in the absence of LFC. In particular, generalized bistability can be obtained between either a chaotic or a periodic regime and the off state.

II. LASER EQUATIONS

The local-field correction is needed when dipole-dipole interactions become non-negligible, typically in a dense medium. It has been demonstrated that dipole-dipole interactions lead to a renormalization of the detuning in the Bloch equations [12,15]. This renormalization is dependent on the population inversion. According to this approach, the modi-

*Present address: CIRIL-ISMRA, 6 Blvd. Maréchal Juin, 14050 Caen Cedex 4, France.
†Electronic address: sanchez@coria.fr

fied Maxwell-Bloch equations can be written [10,13,15]

$$\frac{\partial d}{\partial \tau} = -\gamma[d - r + \tfrac{1}{2}(ep^* + e^* p)],$$

$$\frac{\partial p}{\partial \tau} = -[1 - i(\delta - bd)]p + ed, \tag{1}$$

$$\frac{\partial e}{\partial \tau} = -\sigma(e - p),$$

where

$$e = \frac{2\mu}{\hbar\sqrt{\gamma_\parallel \gamma_\perp}}\mathcal{E},$$

$$d = \frac{\omega N_0 \mu^2}{\hbar \epsilon_0 \gamma_\perp \gamma_I} D,$$

$$p = i\frac{2\omega N_0 \mu^2}{\hbar \epsilon_0 \gamma_I \sqrt{\gamma_\parallel \gamma_\perp}} P.$$

D is the population inversion, P and $\mathcal{E}$ are the complex amplitudes of the macroscopic polarization and the electric field, respectively. μ is the dipole moment. $\gamma_\parallel$, $\gamma_\perp$, and γ_I are the relaxation constants of the inversion, the polarization, and the optical intensity, respectively. N_0 is the density of dipoles. ω is the electric field frequency. $\delta = (\omega - \omega_0)/\gamma_\perp$ is the normalized frequency detuning referenced to the atomic line-center frequency ω_0. r represents the pumping parameter. The time τ is normalized to the coherence lifetime ($\tau = \gamma_\perp t$). The other parameters are $\sigma = \gamma_I/(2\gamma_\perp)$ and $\gamma = \gamma_\parallel/\gamma_\perp$. The parameter b is related to dipole-dipole interactions [13]. It is real and positive. Throughout this paper we take $\sigma = 3$ and $\gamma = 1$ for the numerical calculations in order to compare with previously published results related to the laser equations in the absence of local-field correction [2,3,10]. These values allow one to achieve unstable steady states and physically correspond to the so-called bad-cavity configuration where the photon lifetime is lower than both the dipole lifetime and the inversion lifetime.

For the investigation of the steady-state solutions and for numerical integration we write Eq. (1) in a more convenient form. Let us first consider the transformation into real and imaginary parts:

$$e = x_1 + ix_2, \quad p = x_3 + ix_4, \quad d = x_5. \tag{2}$$

We now define new dynamical variables:

$$I = x_1^2 + x_2^2, \quad P = x_3^2 + x_4^2, \quad C = x_1 x_3 + x_2 x_4,$$
$$D = x_1 x_4 - x_2 x_3, \quad X = x_5. \tag{3}$$

I represents the laser intensity, P the square of the amplitude of the macroscopic polarization, and X the population inversion. The remaining variables C and D have no physical meaning, they just naturally appear in the dynamical equations with I, P, and X.

System (1) becomes

$$\dot{I} = -2\sigma(I - C), \quad \dot{P} = -2(P - CX),$$

$$\dot{C} = -(1+\sigma)C + \sigma P + IX - D(\delta - bX), \tag{4}$$

$$\dot{D} = -(1+\sigma)D + C(\delta - bX), \quad \dot{X} = -\gamma(X - r + C),$$

where the overdot stands for the time derivative. The phase space spanned by (I, P, C, D, X) is quite well adapted to representation of the different attractors (limit cycles or strange attractors).

Let us now consider some symmetry properties of system (4). When $b = 0$, it can easily be shown that if δ is replaced by $-\delta$, then system (4) is unchanged provided that D is replaced by $-D$. This means that the dynamics can be studied only for $\delta \geqslant 0$ [2,19]. Therefore, this symmetry restricts the range of investigation. The problem is different when $b \neq 0$ because this symmetry is not valid. As a consequence, we have to investigate system (4) for both positive and negative values of δ. The dynamics is expected to be different for positive or negative frequency detunings.

III. STATIONARY STATES

At steady state, all the derivatives vanish and system (4) admits three fixed points: (i) the off state

$$(\overline{I}_o = 0,\ \overline{P}_o = 0,\ \overline{C}_o = 0,\ \overline{D}_o = 0,\ \overline{X}_o = r) \tag{5}$$

where the bar stands for the steady-state values, and (ii) two lasing states,

$$\begin{pmatrix} \overline{I}_\pm = r - r_{\mathrm{th}\pm} \\ \overline{P}_\pm = r_{\mathrm{th}\pm}(r - r_{\mathrm{th}\pm}) \\ \overline{C}_\pm = r - r_{\mathrm{th}\pm} \\ \overline{D}_\pm = \dfrac{1}{1+\sigma}(r - r_{\mathrm{th}\pm})(\delta - b r_{\mathrm{th}\pm}) \\ \overline{X}_\pm = r_{\mathrm{th}\pm} \end{pmatrix}, \tag{6}$$

where $r_{th\pm}$ are the lasing thresholds of the two lasing solutions,

$$r_{\mathrm{th}\pm} = \frac{1}{2b^2}\{2b\delta + (1+\sigma)^2 \pm \sqrt{(1+\sigma)^2[(1+\sigma)^2 + 4b(\delta - b)]}\}. \tag{7}$$

Let us note that the lowest threshold solution gives the usual solution of a detuned homogeneously broadened laser in the limit where $b \to 0$, whereas the highest threshold solution diverges [10]. Thus, in the absence of dipole-dipole interactions, there remains only one lasing solution as expected. In

the following, we will call the lower and higher modes (or solutions), the solutions of lowest and highest lasing threshold, respectively.

It is well known that, when $b=0$, the lasing threshold is a symmetric curve versus the frequency detuning δ [2]. We have demonstrated in [10] that for $b>0$ the curve is globally shifted and the symmetry versus δ is broken. However, the minimum threshold operation remains unchanged.

IV. LINEAR STABILITY ANALYSIS

A. Stability of the off state

Let us define small perturbations from the off state:

$$\delta\vec{U}=\begin{pmatrix}\delta I=I-\overline{I_o}\\ \delta P=P-\overline{P_o}\\ \delta C=C-\overline{C_o}\\ \delta D=D-\overline{D_o}\\ \delta X=X-\overline{X_o}\end{pmatrix}. \tag{8}$$

Assuming that $\|\delta\vec{U}\|\ll 1$, system (4) can be linearized around the steady state and written in the form

$$\delta\dot{\vec{U}}=\underline{L}_o(0)\,\delta\vec{U}, \tag{9}$$

where

$$\underline{L}_o(\lambda)=\begin{pmatrix}-2\sigma-\lambda & 0 & 2\sigma & 0 & 0\\ 0 & -2-\lambda & 2r & 0 & 0\\ r & \sigma & -1-\sigma-\lambda & -(\delta-br) & 0\\ 0 & 0 & \delta-br & -1-\sigma-\lambda & 0\\ 0 & 0 & -\gamma & 0 & -\gamma-\lambda\end{pmatrix} \tag{10}$$

and $\underline{L}_o(0)=\underline{L}_o(\lambda=0)$.

The characteristic polynomial of the eigenvalue problem is defined by $\mathcal{P}_0(\lambda)=\det[\underline{L}_o(\lambda)]$. For the off state, the roots of the polynomial can be analytically evaluated:

$$\begin{aligned}\lambda_0&=-\gamma,\\ \lambda_1&=-1-\sigma-\frac{1}{\sqrt{2}}(\alpha-\sqrt{\beta})^{1/2},\\ \lambda_2&=-1-\sigma+\frac{1}{\sqrt{2}}(\alpha-\sqrt{\beta})^{1/2},\\ \lambda_3&=-1-\sigma-\frac{1}{\sqrt{2}}(\alpha+\sqrt{\beta})^{1/2},\\ \lambda_4&=-1-\sigma+\frac{1}{\sqrt{2}}(\alpha+\sqrt{\beta})^{1/2},\end{aligned} \tag{11}$$

where

$$\begin{aligned}\alpha&=1-2\sigma+\sigma^2+4r\sigma-(\delta-br)^2,\\ \beta&=b^4r^4-4b^3r^3\delta+\delta^4+4br\delta(-1-\delta^2+2\sigma+4r\sigma-\sigma^2)\\ &\quad+2\delta^2[1+\sigma(\sigma-2-4r)]\\ &\quad+2\delta^2[1+3\delta^2+\sigma(\sigma-2-4r)]+[1+\sigma(\sigma-2+4r)]^2.\end{aligned} \tag{12}$$

As to the parameters used, λ_1 and λ_2 are two complex conjugate eigenvalues with negative real parts. λ_0 and λ_3 are both real negative numbers. λ_4 is a real eigenvalue and is negative below the lasing threshold of the lowest mode. It becomes positive above $r_{\mathrm{th}-}$, meaning that the laser starts to oscillate. However, in contrast with the classical complex Lorenz-Haken equations, λ_4 again becomes negative beyond a critical value of the pumping parameter. Figure 1 shows

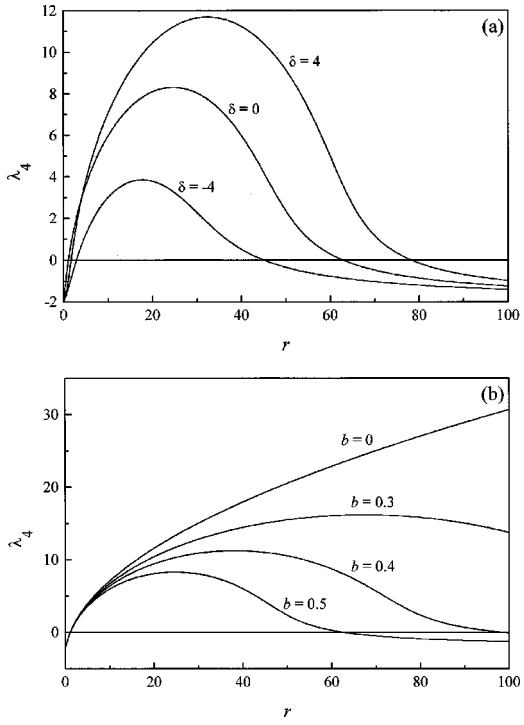

FIG. 1. Evolution of the highest real eigenvalue of the linearized matrix associated with the off state versus the pumping ratio. (a) $b=0.5$ and δ variable. (b) $\delta=0$ and b variable.

examples of the evolution of λ_4 versus r for several detunings and b values. These curves clearly show that when $b \neq 0$ the off state is unstable within a finite range of pumping parameters. This range decreases either when dipole-dipole interactions increase or when the frequency detuning decreases. A straightforward calculation shows that $\lambda_4 = 0$ for $r = r_{\mathrm{th}\pm}$. Therefore the off state becomes stable beyond the lasing threshold of the higher mode. The stability of the off state will be discussed further in Sec. V D.

B. Stability of lasing states

Following the same procedure as in the previous section, the problem can also be formulated in matrix form. We finally obtain the following reduced linearized matrix [10]:

$$\underline{L}_{\pm} = \begin{pmatrix} -\sigma & \sigma & 0 & 0 \\ r_{\mathrm{th}\pm} - \dfrac{\sigma}{(1+\sigma)^2}(\delta - b r_{\mathrm{th}\pm})^2 & -1 & \dfrac{\sigma-1}{\sigma+1}(\delta - b r_{\mathrm{th}\pm}) & \sqrt{I_{\pm}}\left(1 + \dfrac{b}{1+\sigma}(\delta - b r_{\mathrm{th}\pm})\right) \\ \dfrac{\sigma}{1+\sigma}(\delta - b r_{\mathrm{th}\pm}) & \dfrac{1}{1+\sigma}(\delta - b r_{\mathrm{th}\pm}) & -1-\sigma & -b\sqrt{I_{\pm}} \\ -\gamma\sqrt{I_{\pm}} & -\gamma\sqrt{I_{\pm}} & 0 & -\gamma \end{pmatrix}. \quad (13)$$

The stability of the lower solution has been investigated in [10]. The results show that, in the so-called bad-cavity configuration, this solution loses its stability via a Hopf bifurcation for a critical value of the pumping parameter r_c (instability threshold). For the parameters used, the instability threshold is such that $r_{\mathrm{th}+} > r_c > r_{\mathrm{th}-}$. The main result obtained in Ref. [10] is that the minimum instability threshold is reduced when dipole-dipole interactions are taken into account and it does not occur for $\delta = 0$. In addition, the condition required for the instability to occur is

$$\gamma < \frac{2(-1+\sigma)}{1-\sigma+\sqrt{4b(\delta-b)+(1+\sigma)^2}}, \quad (14)$$

which is less restrictive than the condition required in the absence of dipole-dipole interactions, i.e., $\sigma > 1+\gamma$ [2,3].

Figure 2 represents the evolution of r_c versus the detuning for increasing values of b. Figure 3 gives the evolution of the detuning ($\delta_{\min}$) that allows one to achieve a minimum instability threshold as a function of b. These values will be useful in the next section to investigate the dynamics at the minimum instability threshold.

Let us now consider the stability of the higher solution. The characteristic polynomial of the eigenvalue problem can be put in the form

$$\mathcal{P}_+(\lambda) = \det(\underline{L}_+ - \lambda \underline{I}) = (\lambda - \lambda_1)(\lambda - \lambda_2)(\lambda - \lambda_3)(\lambda - \lambda_3^*), \quad (15)$$

where $\underline{I}$ is the identity matrix and the λ_i's are the roots of $\mathcal{P}_+(\lambda)$. For the parameters used ($\sigma = 3$, $\gamma = 1$, $-4 \leqslant \delta \leqslant 4$, $b > 0$, and $r \geqslant r_{\mathrm{th}+}$), $\mathcal{P}_+(\lambda)$ has two complex conjugate eigenvalues (λ_3, λ_3^*) with a negative real part and one real negative eigenvalue (λ_2). The last eigenvalue (λ_1) is real and positive for $r \geqslant r_{\mathrm{th}+}$, meaning that the higher solution loses its stability directly at its lasing threshold. Because at the same time the off state again becomes stable for $r \geqslant r_{\mathrm{th}+}$ and the lower solution is also unstable, the result is that the laser returns to the off state above the lasing threshold of the higher solution.

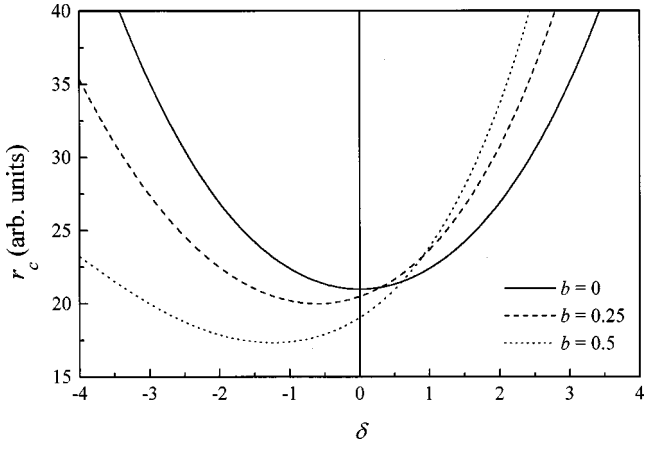

FIG. 2. Evolution of the instability threshold r_c versus δ.

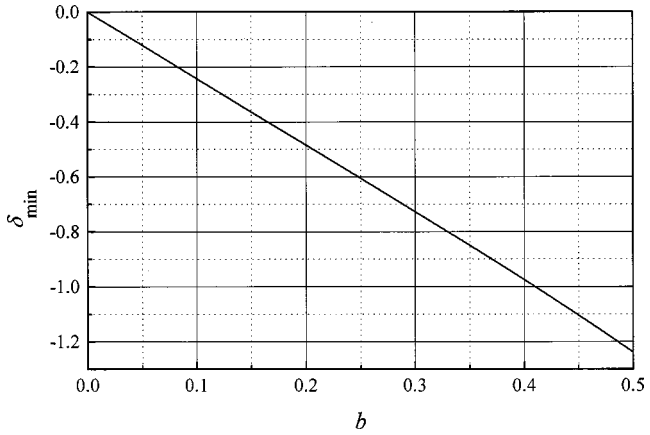

FIG. 3. Evolution of the detuning $\delta_{\min}$ allowing the minimum of r_c versus b.

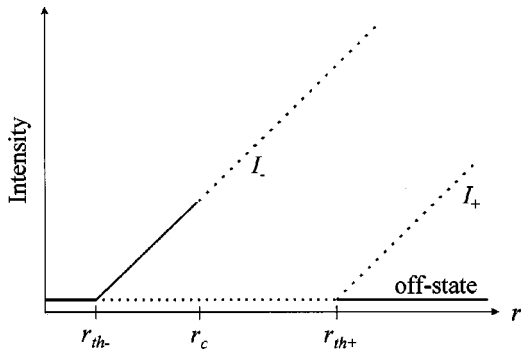

FIG. 4. Schematic representation of the stability of the three solutions as a function of the pumping parameter. The solid lines correspond to stable steady states and the dotted lines to unstable steady states.

The results of our linear stability analysis are summarized in Fig. 4, which gives the stability of the three solutions versus the pumping parameter r. This representation shows that, for the parameters used, no bistability can be achieved in the stationary regime because there is no coexistence of two stable steady-state solutions.

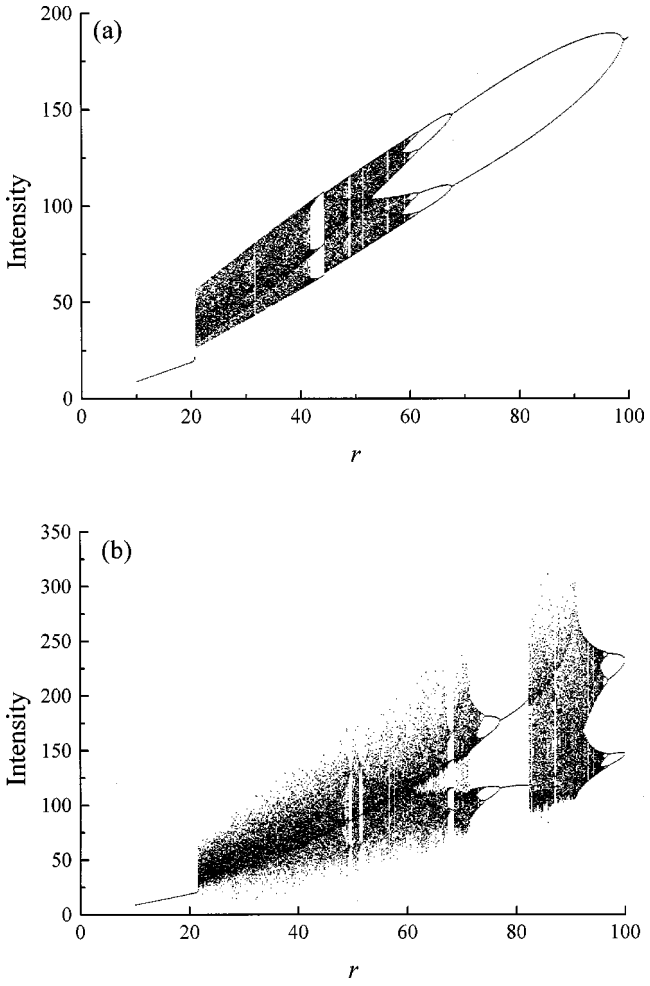

FIG. 5. Bifurcation diagrams versus r. (a) $b=0.25$ and $\delta=-0.652$. (b) $b=0$ and $\delta=0$.

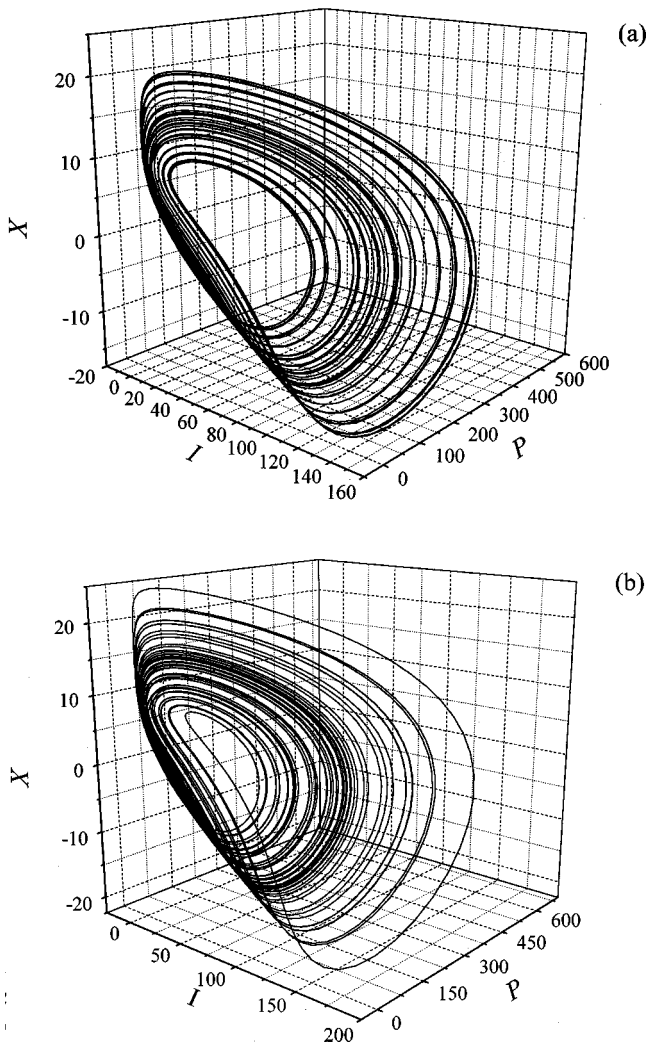

FIG. 6. Chaotic attractor for $r=40$. (a) $b=0.25$ and $\delta=-0.652$. (b) $b=0$ and $\delta=0$.

V. NUMERICAL SOLUTIONS

The results obtained in the stationary regime demonstrate that dipole-dipole interactions are equivalent to an inversion-dependent renormalization of the frequency detuning. In the time-dependent regime, this renormalization is also time dependent, leading to additional nonlinear couplings in the Lorenz-Haken equations. The aim of this section is to identify the differences induced by the local-field correction in the dynamical behavior of a single-mode homogeneously broadened laser. System (4) is numerically solved using a Runge-Kutta method with an adaptative integration step.

A. A first comparison

Figure 5 gives the bifurcation diagrams versus the pumping ratio at the minimum instability threshold for $b=0.25$ and $b=0$, for comparison. In both cases, the system falls into the chaotic regime directly at the instability threshold and undergoes an inverse period-doubling cascade for high pumping rates. In each case, there are periodic windows. Globally, the main difference is a reduction of the chaotic

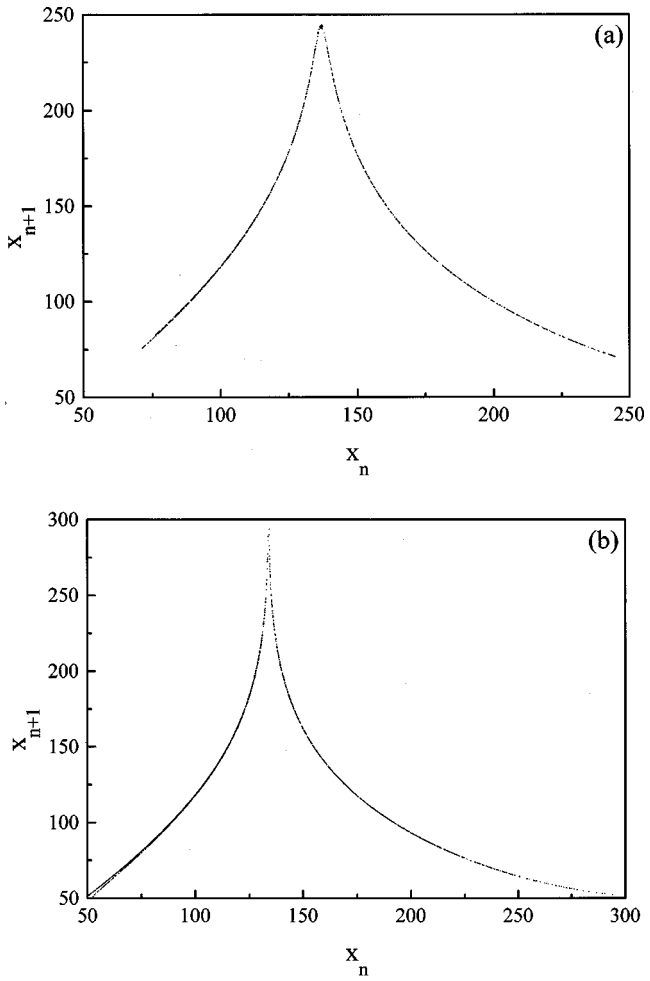

FIG. 7. First-return maps for $r=22$. (a) $b=0.25$ and $\delta=-0.652$. (b) $b=0$ and $\delta=0$.

range when dipole-dipole interactions are taken into account. Further comparison can be made with the help of the chaotic attractors and the first-return maps. Figure 6 represents the chaotic attractors in the phase space (I, P, X) at a value of the detuning allowing minimum instability threshold operation, for $b=0.25$ [Fig. 6(a)] and for $b=0$ [Fig. 6(b)]; the pumping ratio is $r=40$. Figure 7 gives the first-return maps just above the Hopf bifurcation ($r=22$); the other parameters are unchanged. Here again, there is no clear differences between the solutions with and without dipole-dipole interactions. When $b\neq 0$, the strange attractor together with the first-return map are very similar to those of the solution of the Lorenz-Haken equations without the LFC [19].

In the following, we investigate two cases successively. We first globally compare the dynamics at the minimum instability threshold for several b values and then investigate the influence of the frequency detunings for a fixed value of b. Owing to the renormalization of the detuning, one can reasonably expect that the dynamics at the minimum instability threshold will not be globally changed, while detuning effects will induce noticeable differences with respect to the solution of the complex Lorenz-Haken equations.

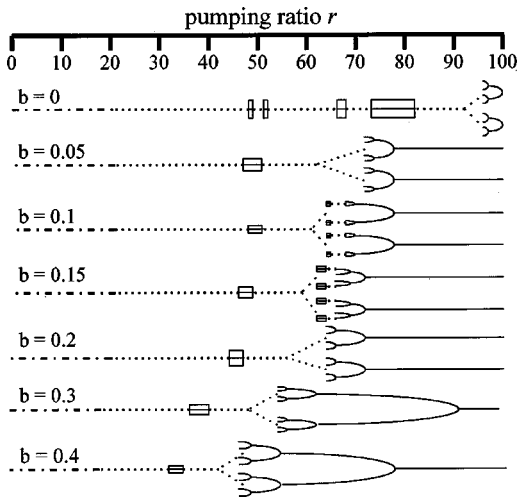

FIG. 8. Bifurcation diagram at the minimum instability threshold for increasing values of b. Dashed-dotted lines correspond to stable steady states, dotted lines to chaotic regimes, small boxes with solid lines to periodic windows within the chaotic regime, and solid lines to periodic solutions. In the latter case, one line corresponds to a C^1 periodic orbit, two lines to a C^2, and so on.

B. Dynamics at the minimum instability threshold

We use here the results of Fig. 3 in order to compute the bifurcation diagrams at the minimum instability threshold for b ranging from 0 to 0.4. Figure 8 schematically represents the bifurcation diagrams when the pumping parameter is

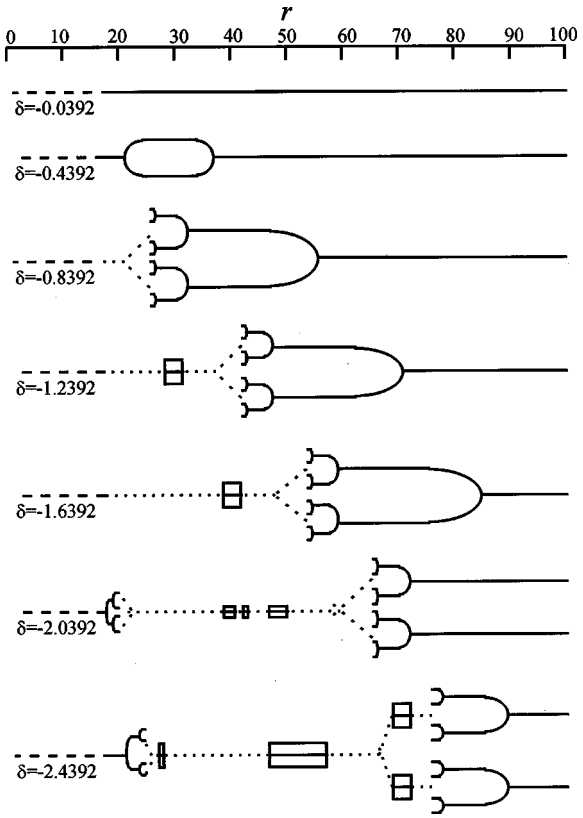

FIG. 9. Bifurcation diagram versus δ for $b=0.5$. Same conventions as in Fig. 8.

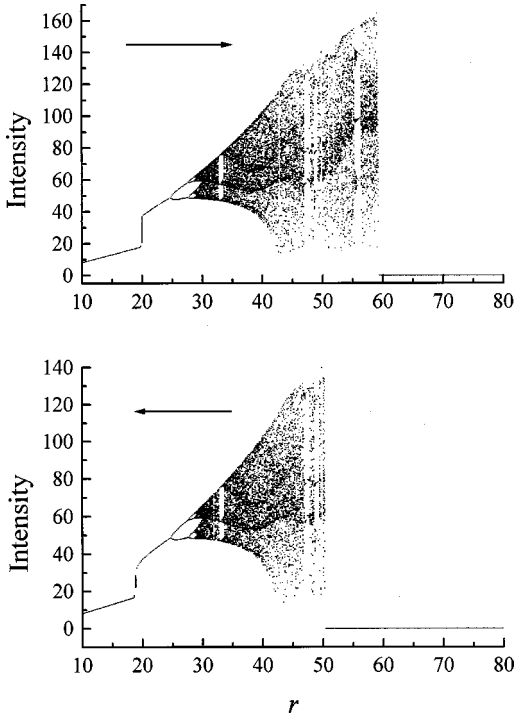

FIG. 10. Bifurcation diagram for increasing and decreasing pumping rates in the case of large frequency detunings. $b=0.5$ and $\delta=-2.8392$.

adiabatically increased. There are no qualitative changes on the dynamics. Indeed, for any value of b, the laser is stable for $r_{\mathrm{th}-}<r<r_c$; at $r=r_c$, the system falls directly into a chaotic regime through a Hopf bifurcation. Finally, beyond a second critical value of r, the system follows an inverse Feigenbaum sequence. The effect of the local-field correction on the dynamics, at the minimum instability threshold, is a global reduction of the chaotic domain.

C. Influence of the detuning

Figure 9 shows the influence of the frequency detuning on the dynamical behavior of the laser in the case where $b=0.5$. In this case, the minimum instability threshold is achieved for $\delta_{\min}=-1.2392$. In the following, we will take this value as the reference. In contrast to the classical Lorenz-Haken model [2], the symmetry versus the detuning is broken. Indeed, the evolution is different depending on the sign of the detuning referenced to $\delta_{\min}$. The chaotic domains increase when the detuning is shifted to the left of $\delta_{\min}$ (negative values). On the other hand, when δ is tuned toward positive values starting from $\delta_{\min}$, the evolution is similar to that obtained in the absence of dipole-dipole interactions [2]. Indeed, in the latter case, the detuning tends to stabilize the chaotic regime onto periodic orbits of low order. Finally, far from $\delta_{\min}$ the system stabilizes on a limit cycle of period 1 for any pumping rate above the instability threshold. When δ is tuned toward negative values starting from $\delta_{\min}$, the chaotic domain increases and there is the emergence of a period-doubling cascade before the chaotic regime. At the same time, large periodic windows appear within the chaotic domain. This is the opposite result to the one obtained in the absence of local-field correction, where the emergence of a period-doubling cascade is accompanied by a reduction of the range of pumping rates for which the system is chaotic [2]. In addition, no periodic windows within this range have been reported. Our results essentially demonstrate that, from the dynamical point of view, the local-field correction is not a simple renormalization of the frequency detuning.

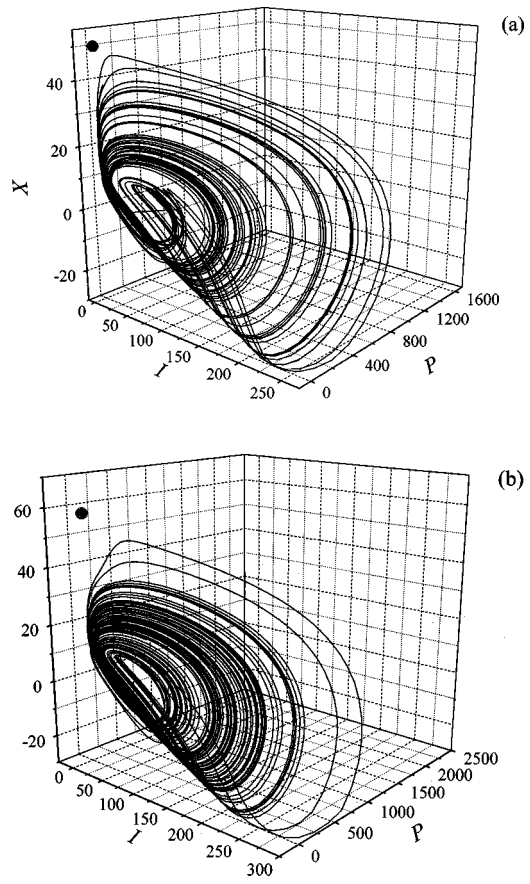

FIG. 11. Chaotic attractor for $b=0.5$ and $\delta=-2.8392$. (a) $r=50$ and (b) $r=58$. The gray circle represents the off state.

D. Generalized bistability

Up to now we have not observed the switch of the laser toward the stable off state above $r_{\mathrm{th}+}$. For example, in Fig. 9, in the case $\delta=-2.4392$, the laser should have returned to the off state for a pumping ratio of about 50. Numerical simulations do not point out this expected switch. This fact suggests the existence of a range of generalized bistability between unstable steady states and the off state. This bistability arises as a consequence of the smallness of the basins of attraction of the off state in the region $r\geqslant r_{\mathrm{th}+}$. In order to confirm the bistability we have calculated the bifurcation diagram for increasing and decreasing pumping rates. The results are given in Fig. 10 for $b=0.5$ and $\delta=-2.8392$, and clearly exhibit a large bistability domain between a chaotic attractor and a fixed point. It is not trivial to determine the basins of attraction of the off state because the system evolves in a five-dimensional space. Nevertheless, we have verified that, for $r\geqslant r_{\mathrm{th}+}$, if we take as initial conditions a

perturbed off state, the laser systematically falls into the basins of attraction of the chaotic solution as the perturbation is increased. Further investigation of the bifurcation diagrams for increasing and decreasing pumping rates has shown that the expected switch never occurs for δ greater than about -2.5. No generalized bistability has been observed under these conditions for pumping ratios up to $r=150$. The absence of the switch implies that the different attractors of the system (strange attractor or periodic orbits) do not pass through the basins of attraction of the off state. Therefore, the system cannot be attracted by the stable off state. One can give some physical insight into the influence of the detuning on the switches. Figures 11(a) and 11(b) show the attractors for $b=0.5$, $\delta=-2.8392$, and $r=50$ and 58, respectively. The off state is also represented. The trajectory in the phase space approaches the off state each time the population inversion is high. For large negative values of δ, the trajectory passes very close to the off state. The instantaneous frequency detuning $\delta-bX$ of the modified Maxwell-Bloch equations then becomes very negative. In some cases, this instantaneous detuning becomes so negative that the laser can no longer oscillate. A switch to the off state occurs. For either moderate negative or positive detunings, the trajectory remains far from the off state. The instantaneous detuning is never very large and the laser continues to oscillate; no switch occurs.

Figure 10 also exhibits a bistability between the stationary state and a periodic orbit near the instability threshold r_c. In addition, the curve shows that the bifurcation is subcritical for the parameters used. These two features have been observed previously in the classical detuned homogeneously broadened laser equations [3], i.e., in absence of the LFC.

VI. CONCLUSIONS

The influence of the local-field correction on the dynamics of a single-mode homogeneously broadened laser has been investigated. The five-dimensional system of equations admits three fixed points: the off state and two lasing states. A linear stability analysis has revealed that the off state is unstable within a finite range of pumping rates, spanning from the lasing threshold of the lower solution ($r_{\mathrm{th}-}$) to the lasing threshold of the higher solution ($r_{\mathrm{th}+}$). The lower solution is stable between $r_{\mathrm{th}-}$ and a critical value r_c, at which the stability is lost through a Hopf bifurcation. The higher solution is always unstable. Therefore, the LFC tends to stabilize the off state above a particular value of the pumping parameter. The numerical simulations have pointed out important differences between the dynamical scenarios with and without local-field correction. First, we have demonstrated that, at the minimum instability threshold, the LFC reduces the range of chaotic operation. For a given LFC parameter, the symmetry versus the frequency detuning is broken. Hence, from the dynamical point of view, the LFC is not a simple renormalization of the frequency detuning. In addition, the LFC induces generalized bistability for large negative frequency detunings.

[1] H. Haken, Phys. Lett. **53A**, 77 (1975).
[2] H. Zeghlache and P. Mandel, J. Opt. Soc. Am. B **2**, 18 (1985).
[3] C-Z. Ning and H. Haken, Phys. Rev. A **41**, 3826 (1990).
[4] H. Gang, C.-Z. Ning, and H. Haken, Phys. Rev. A **41**, 3975 (1990).
[5] P. Mandel and H. Zeghlache, Opt. Commun. **47**, 146 (1983).
[6] A. A. Bakasov and N. B. Abraham, Phys. Rev. A **48**, 1633 (1993).
[7] M. J. Tomas, E. Roldan, G. J. De Valcarcel, and R. Vilaseca, Opt. Commun. **114**, 111 (1995).
[8] A. C. Fowler, J. D. Gibbon, and M. J. McGuinness, Physica D **4**, 139 (1982).
[9] L. W. Casperson, Phys. Rev. A **21**, 911 (1980).
[10] F. Sanchez, M. Brunel, G. Martel, and K. Aït Ameur, Phys. Rev. A **61**, 033817 (2000).
[11] F. A. Hopf, C. M. Bowden, and W. H. Louisell, Phys. Rev. A **29**, 2591 (1984).
[12] Y. Ben-Aryeh, C. M. Bowden, and J. C. Englund, Phys. Rev. A **34**, 3917 (1986).
[13] A. A. Afanas'ev, R. A. Vlasov, N. B. Gubar, and V. M. Volkov, J. Opt. Soc. Am. B **15**, 1160 (1998).
[14] Y. Ben-Aryeh, C. M. Bowden, and J. C. Englund, Opt. Commun. **61**, 147 (1987).
[15] C. M. Bowden and P. Dowling, Phys. Rev. A **47**, 1247 (1993).
[16] J. W. Haus, L. Wang, M. Scalora, and C. M. Bowden, Phys. Rev. A **38**, 4043 (1988).
[17] M. Brunel, C. Özkul, and F. Sanchez, J. Opt. Soc. Am. B **16**, 1886 (1999).
[18] C. M. Bowden, S. Sing, and G. P. Agrawal, J. Mod. Opt. **42**, 101 (1995).
[19] C. O. Weiss and R. Vilaseca, *Dynamics of Lasers*, Vol. 1 of *Nonlinear Systems* (VCH, Weinheim, 1991).
[20] J. D. Crawford, Rev. Mod. Phys. **63**, 991 (1991).
[21] G. Iooss and D. D. Joseph, *Elementary Stability and Bifurcation Theory*, *Undergraduate Texts in Mathematics*, 2nd ed. (Springer-Verlag, New York, 1990).